View metadata, citation and similar papers at core.ac.uk
brought to you by CORE
provided by Helsingin yliopiston digitaalinen arkisto

Piperazine Enhancing Sulfuric Acid Based New Particle Formation: Implications for the Atmospheric Fate of Piperazine

Fangfang Ma[†], Hong-Bin Xie[†*], Jonas Elm[‡], Jiewen Shen[†], Jingwen Chen[†*] and Hanna Vehkamäki[§]

[†]Key Laboratory of Industrial Ecology and Environmental Engineering (Ministry of Education), School of Environmental Science and Technology, Dalian University of Technology, Dalian 116024, China

[‡]Department of Chemistry and iClimate, Aarhus University, Langelandsgade 140, DK-8000 Aarhus C, Denmark

[§]Institute for Atmospheric and Earth System Research/Physics, University of Helsinki, PO Box 64 (Gustaf Hällströmin katu 2a), FI-00014 Helsinki, Finland

Table of Contents (TOC)

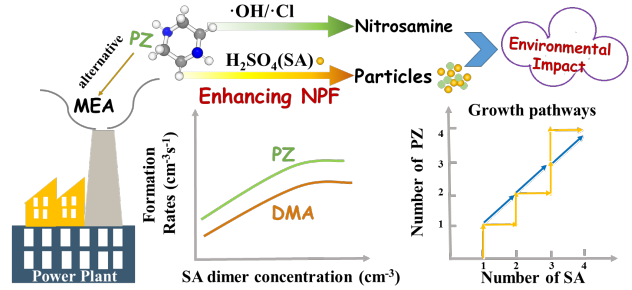

MEA: Monoethanolamine; PZ: Piperazine; DMA: dimethylamine; NPF: New Particle Formation

ABSTRACT: Piperazine (PZ), a cyclic diamine, is one of 160 detected atmospheric amines and an alternative solvent to the widely used monoethanolamine in post-combustion CO_2 capture. Participating in H_2SO_4 (SA)-based new particle formation (NPF) could be an important removal pathway for PZ. Here, we employed quantum chemical calculations and kinetics modeling to evaluate the enhancing potential of PZ on SA-based NPF by examining the formation of PZ–SA clusters. The results indicate that PZ behaves more like a monoamine in stabilizing SA and can enhance SA-based NPF at the parts per trillion (ppt) level. The enhancing potential of PZ is less than that

of the chainlike diamine putrescine, and greater than that of dimethylamine which is one of the strongest enhancing agents confirmed by ambient observations and experiments. After the initial formation of the $(PZ)_1(SA)_1$ cluster, the cluster mainly grows by gradual addition of SA or PZ monomer, followed by addition of $(PZ)_1(SA)_1$ cluster. We find that the ratio of PZ removal by NPF to that by the combination of NPF and oxidations is 0.5-0.97 at 278.15 K. As a result, the participation in the NPF pathway could significantly alter the environmental impact of PZ compared to only considering oxidation pathways.

INTRODUCTION

Amines are a class of atmospheric nitrogen-containing organic pollutants. Up to now, about 160 different amines have been detected in the atmosphere.[1] Amines are emitted into the atmosphere from both natural and anthropogenic sources including agriculture, biomass burning, animal husbandry, oceans, cooking, smoking and various industrial processes.[1-12] It deserves mentioning that CO_2 capture units will become a significant source of amines once the promising amine-based CO_2 capture technology is implemented on a large scale.[13-15] In recent years, the concern about the fate of amines has been increasing since the transformation of amines could potentially form carcinogenic nitrosamines.[1]

Several studies have addressed the removal of amines by atmospheric oxidation.[16-39] The oxidation by hydroxyl radicals (·OH) has been considered to be their main transformation pathway, followed by chlorine radicals (·Cl), at daytime.[18,32] The reactions with ·OH and ·Cl lead to amines having an atmospheric lifetime on the order of hours.[1,13,17-19,22-28,32] More importantly, the atmospheric oxidation by ·OH and ·Cl can lead to the formation of N-center radicals, which can further react with NO_x (x = 1, 2) to form hazardous nitrosamines/nitramine (Scheme 1), increasing the environmental

risk of the amines emissions.[17,18,28,30,32] Although the direct reaction of amines with NO_x can also lead to the formation of nitrosamines, several studies have shown that it is of little importance under atmospheric condition.[13,40,41] Besides oxidation reactions, many studies have found that amines such as monomethylamine (MA), dimethylamine (DMA), trimethylamine (TMA) and monoethanolamine (MEA) can significantly enhance H_2SO_4 (SA)-based new particle formation (NPF) via acid-base reactions, an important process for the formation of atmospheric aerosol particles.[42-72] However, there are few studies concerning how the participation of amines in SA-based NPF competes with their oxidation pathways and thereby affects the fate of atmospheric amines. Our recent study indicated that the participation in SA-based NPF is an important sink for MEA, and it could even be comparable to the oxidation reaction pathway initiated by ·OH at 278.15 K.[70] This implies that the participation in NPF could be a significant pathway in determining the fate of other amines, especially those with high enhancing potential for SA-based NPF.

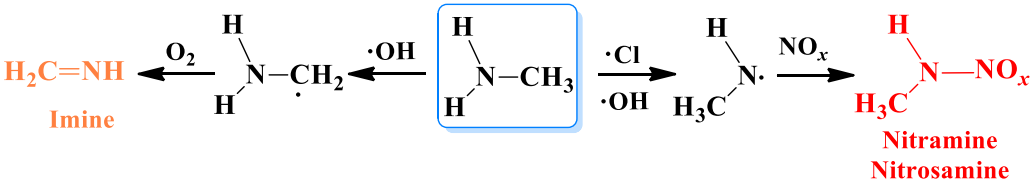

Scheme 1. Major reaction pathways for ·OH/·Cl initiated reactions of amines. Here exemplified using methylamine.

Piperazine (PZ), a cyclic secondary diamine, whose aqueous solution is considered an alternative solvent to MEA, a benchmark and widely used solvent in post-combustion CO_2 capture (PCCC) technology.[73,74] Once PZ-based PCCC technology is implemented on a large scale, quantities of PZ might be released into the atmosphere from PCCC units due to its relatively high vapor pressure.[75] PZ has previously been identified as one of the 160 amines detected in the ambient atmosphere.[1] In Zonguldak

province, Turkey, the concentration of PZ was found to reach about 4 parts per trillion (ppt), which is higher than that of DMA (about 1 ppt) at the same location.[76] Our recent study showed that the daytime atmospheric oxidation of PZ initiated by ·OH and ·Cl can lead to higher yield of carcinogenic nitrosamines compared to the corresponding oxidation process of MEA, implying higher environmental risk related to PZ than MEA emissions.[32] Similar to MEA,[70] the participation of PZ in SA-based NPF via acid-base reactions could be a significant pathway to compete with its oxidation pathways. However, to the best of our knowledge, there are currently no studies that address the participation of PZ in SA-based NPF.

The gas phase basicity (GB) of amines has been suggested to be an important parameter in determining their enhancing potential on SA-based NPF.[53,54] The GB value of PZ (914.7 kJ mol^{-1}) is significantly higher than those of previously studied monoamines and ammonia (MA 864.5, DMA 896.5, MEA 896.8, NH_3 819.0 kJ mol^{-1}).[77] Therefore, based purely on the GB, PZ should have much higher enhancing potential on SA-based NPF than NH_3, MA, DMA and MEA under the assumption that they have similar atmospheric concentration. In addition, the steric effect of the –NH– group in the cyclic PZ should be different from previously studied chainlike amines,[56,70,78] which could influence its enhancing potential. At last, if the two –NH– groups of PZ can synergistically interact with SA like chainlike diamine putrescine (PUT), PZ could have much higher enhancing potential than what is expected by its GB. However, due to its rigid cyclic structure, it is not easy to judge whether the two –NH– groups of PZ can synergistically interact with SA. All in all, it is difficult to estimate the enhancing potential of PZ on SA-based NPF based on chemistry intuition. In addition, no previous studies have investigated the potential role of ***cyclic*** diamines in SA-based NPF. Thus, to comprehensively understand the atmospheric fate of PZ and

expand the knowledge of amines enhancing SA-based NPF, it is indispensable to investigate the participation of PZ in SA-based NPF.

Here, we investigated the initial step of PZ participating in SA-based NPF by examining the formation of $(PZ)_x(SA)_y$ (x = 0−4, y = 0−4) clusters by a combined method using quantum chemical calculations with the Atmospheric Cluster Dynamics Code (ACDC)[79-82]. The results are compared with previous studies on the DMA−SA, MEA−SA and PUT−SA systems. In addition, the effect of adding water molecules to the clusters was also considered to study the effect of hydration on the cluster formation kinetics of PZ and SA molecules.

COMPUTATIONAL DETAILS

Configurational Sampling and Electronic Structure Calculations. Obtaining a good estimate of the global free energy cluster structures remains a large challenge in modelling atmospheric NPF. Here, we employed a multi-step sampling scheme to search for the global minima of the $(PZ)_x(SA)_y$ (x = 0−4, y = 1−4) clusters. The pure $(SA)_{1-4}$ clusters were taken from previous work.[81] The multi-step sampling scheme has extensively been applied to study atmospheric cluster formation.[70,78,83-88] In brief, the scheme includes the following six steps: (1) Large number of initial cluster configurations (about 10000 for most of clusters) are randomly generated; (2) All the configurations are initially optimized using the semiempirical PM6 method; (3) Single point energy calculations at the ωB97X-D/6-31+G(d) level of theory is performed on all the optimized configurations; (4) The identified lowest energy configurations within 10-15 kcal mol^{-1} are fully optimized at the ωB97X-D/6-31++G(d,p) level of theory, followed by a vibrational frequency calculation; (5) For the identified lowest free energy configurations (within 1-2 kcal mol^{-1} of the global minimum), the single point energy was refined with a DLPNO-CCSD(T)/aug-cc-pVTZ calculation; (6) Several of

120 the lowest free energy configurations (about 10 for most of clusters) are subsequently
121 used to build initial configurations for the larger clusters starting over from (1). The
122 initial PZ conformations for building the $(PZ)_1(SA)_1$ and $(PZ)_2$ clusters were obtained
123 from our previous AIMD simulation.[32] All geometry optimization, vibrational
124 frequency calculations and single point energies using the PM6 and ωB97X-D methods
125 were performed in the GAUSSIAN 09 program package.[89] The DLPNO-CCSD(T)/aug-
126 cc-pVTZ calculation was performed in the ORCA 4.0.0 program.[90] The ωB97X-D/6-
127 31++G(d,p) and DLPNO-CCSD(T)/aug-cc-pVTZ methods were selected as the core
128 optimization/frequency and single point energy calculations, respectively, since they
129 have shown good performance for studying the formation of atmospheric molecular
130 clusters.[70,91,92] The Gibbs free energy (G) of the identified clusters were calculated at
131 298.15 K with the following formula:

132 $$G = E + G_{corr} \quad (1)$$

133 where E is the electronic single point energy at the DLPNO-CCSD(T)/aug-cc-pVTZ
134 level of theory and G_{corr} is the Gibbs free energy correction at the ωB97X-D/6-
135 31++G(d,p) level of theory. The formation free energy (ΔG) for each cluster at 298.15
136 K was calculated by:

137 $$\Delta G = G_{cluster} - \Sigma G_{monomer} \quad (2)$$

138 where $G_{cluster}$ and $G_{monomer}$ is the free energy of the cluster and the constituent molecules,
139 respectively. The ΔG values at other temperatures were calculated under the assumption
140 that enthalpy (ΔH) and entropy (ΔS) change remain constant in the tropospheric
141 temperature range. It is important to note that the ΔG values of the cluster systems used
142 as a comparison (MEA−SA, DMA−SA, PUT−SA), were obtained at the same
143 theoretical level as those in this study. The Cartesian coordinates of the stable PZ−SA

clusters were presented in the Supporting Information (SI).

To investigate the effect of hydration, we studied the $(PZ)_x(SA)_yW_z$ (x = 0−2, y = 0−2, z = 1−5, "W" represents H_2O) clusters. The $(SA)_1W_{1\text{-}5}$ and $(SA)_2W_{1\text{-}3}$ clusters were taken from previous studies.[70,93] The global minima of $(SA)_2W_{4\text{-}5}$ and $(PZ)_{1\text{-}2}(SA)_{1\text{-}2}W_{1\text{-}5}$ clusters were identified by the same sampling scheme that was used for the unhydrated PZ−SA clusters.

Atmospheric Clusters Dynamic Code (ACDC) Model. The time evolution of formation rates, steady-state concentrations and growth paths of clusters were studied using the ACDC code. The detailed theory of the ACDC can be seen in a previous study.[81] Here, the simulation system was treated as a "4 × 4" box for the unhydrated PZ−SA system, where 4 is the maximum number of PZ or SA molecules of the clusters. The mobility diameter of the largest cluster is ~1.5 nm, which closely resembles the sizes of clusters that can be deemed stable against evaporation in the ambient atmosphere. The $(PZ)_4(SA)_5$ and $(PZ)_5(SA)_5$ clusters were set as the boundary clusters (SI). The ACDC simulations were mainly performed at 278.15 K. In addition, to probe the temperature effect, we also conducted simulations at other temperatures such as 258.15, 268.15, 288.15, 298.15 and 313.15 K. The concentration of SA ([SA]) and PZ ([PZ]) were set to be 10^5, 10^6, 10^7 and 10^8 cm^{-3} (a range relevant to atmospheric particle formation)[62,94-97] and 1, 10, 100 ppt (partly higher than that (about 4 ppt) measured in Zonguldak province, Turkey),[76] respectively. To consider external losses, a constant coagulation sink coefficient of 2.6×10^{-3} s^{-1} was used.[98,99] When studying the effect of hydration, the simulation system was treated as a "2 × 2" box. The [SA] and [PZ] were set to be 10^6 cm^{-3} and 10 ppt, respectively, and the simulations were performed at 278.15 K. The equilibrium hydrate distribution for each cluster was calculated by the equilibrium constant for the formation of the respective hydrate.[88,93,100] The $(PZ)_2(SA)_3$

and $(PZ)_3(SA)_3$ clusters were set as the boundary clusters for the hydrated system.

RESULTS AND DISCUSSION

Cluster Structures. Since many previous studies have already discussed the structures of pure SA clusters,[81] herein, we mainly focus on the clusters $(PZ)_x(SA)_y$ (x = 0−4, y = 1−4). The structures of $(PZ)_x(SA)_y$ (x = 0−4, y = 1−4) clusters with the lowest Gibbs free energy were presented in Figure 1 and the number of the proton transfer observed in the PZ-SA clusters were shown in Table S2. For the homomolecular PZ clusters, proton transfer is not observed and all the clusters except $(PZ)_2$ are mainly stabilized by hydrogen bonds (H-bonds), similar to the cases of studied homomolecular NH_3 or amines clusters.[56,58,59,69,70,78,101,102] However, the $(PZ)_2$ cluster is stabilized by two N···HC interactions. For heteromolecular PZ−SA clusters, proton transfer is observed in all cases and the clusters are stabilized by H-bonds and ionic electrostatic interactions. The proton transfer involves two different patterns. In the first pattern, only one proton of SA is transferred. Therefore, the formation of sulfate ion (SO_4^{2-}) is not observed. In this pattern, PZ can accept one proton in two different ways: 1) one PZ molecule only accepts a single proton. The clusters following this way include $(PZ)_1(SA)_{1\text{-}3}$, $(PZ)_2(SA)_{1\text{-}4}$, $(PZ)_3(SA)_1$ and $(PZ)_3(SA)_3$. Therefore, only one –NH– group of PZ is protonated for these clusters. 2) one PZ molecule accepts two protons from different SA molecules. Therefore, the two –NH– groups of one PZ are protonated. This phenomenon is only observed in the $(PZ)_1(SA)_4$ cluster.

In the second pattern, one SA molecule transfers two protons to two different PZ molecules, resulting in the formation of a SO_4^{2-} and a single protonated –NH– group in the two PZ molecules, as seen in the $(PZ)_4(SA)_{1\text{-}4}$, $(PZ)_3(SA)_2$, and $(PZ)_3(SA)_4$ cluster structures. In the $(PZ)_3(SA)_4$ and $(PZ)_4(SA)_4$ clusters, two and one SA molecules do not transfer any proton, respectively, which makes the number of SA molecules that donate

194 a proton less than the number of protonated PZ. Therefore, one SA in these two clusters
195 has to donate two protons leading to the formation of a SO_4^{2-}. These patterns are vastly
196 different from previously reported amines (MA, MEA, DMA and PUT) and SA clusters
197 with the same composition of acid-base molecules.[69,70,78] Note that the maximum
198 number of formed SO_4^{2-} is one in all considered clusters, in contrast to the clusters
199 consisting of SA and chainlike diamine PUT, in which several SO_4^{2-} can be formed.[78]
200 The difference results from the fact that it is unfavorable for the rigid structure of PZ to
201 simultaneously accept two protons from one SA as opposed to chainlike diamines such
202 as PUT. Therefore, from a structural point of view, PZ behaves more like a monoamine
203 in stabilizing SA. Another structural feature in all the clusters except $(PZ)_1(SA)_4$ is that
204 only one of the –NH– groups of PZ interacts with SA or PZ molecule, the remaining –
205 NH– group points towards the outside. Therefore, the two –NH– groups of PZ neither
206 behave like chainlike diamine to accept two protons from one SA, nor like MEA to
207 synergistically interact with SA or another amine molecule via two functional
208 groups.[70,78]

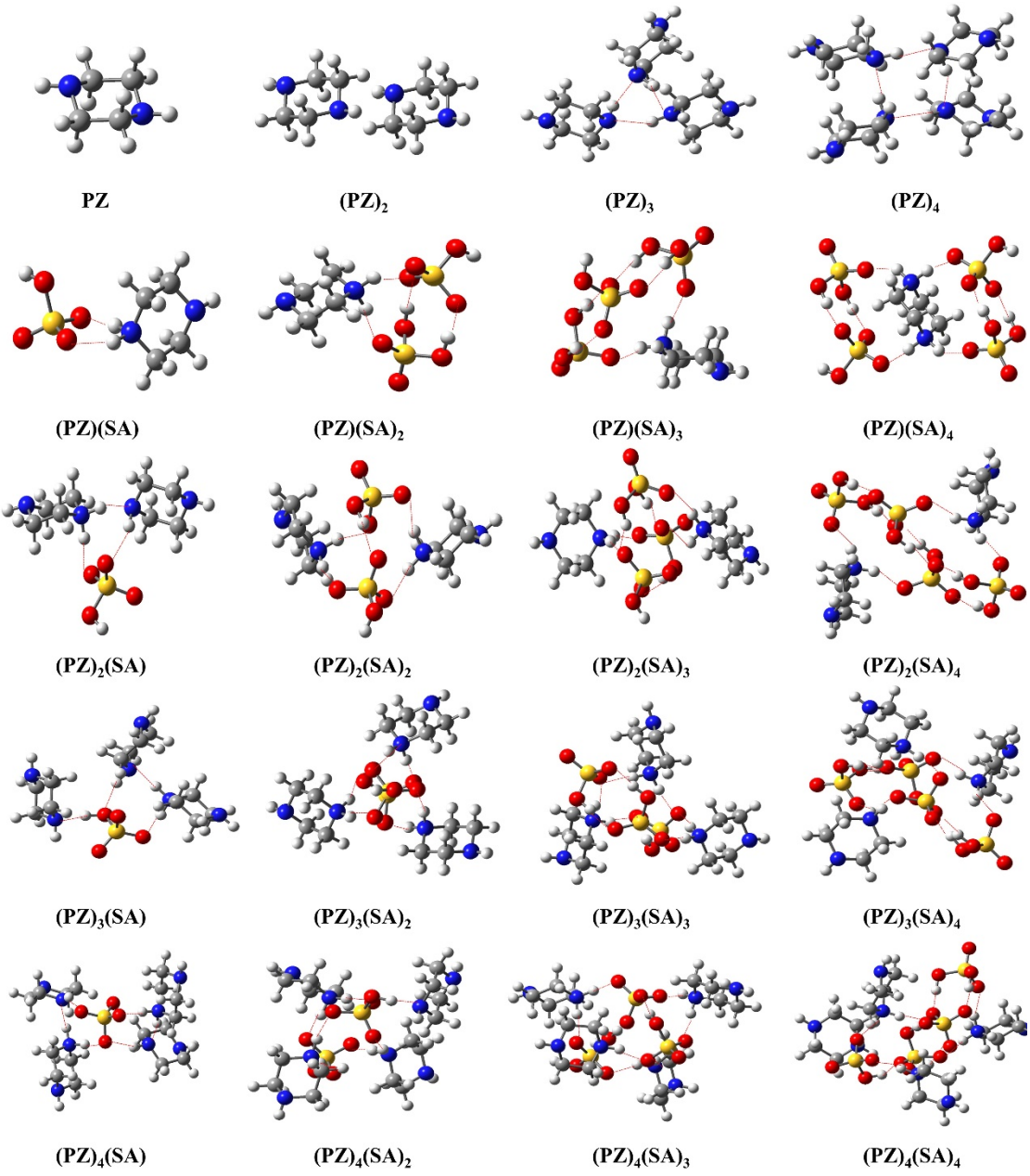

209

210 Figure 1. Identified lowest free energy structures of the $(PZ)_x(SA)_y$ (x = 0−4, y = 1−4)
211 clusters at the ωB97X-D/6-31++G(d,p) level of theory. The red, blue, gray and white
212 balls represent oxygen, nitrogen, carbon and hydrogen atoms, respectively. Dashed red
213 lines indicate hydrogen bonds.

214 **Cluster Formation Free Energy.** Both ambient observations and experimental studies
215 have confirmed that DMA is one of the strongest species for stabilizing SA clusters and
216 thus enhancing NPF.[61,62,71] Therefore, the ΔG values of the DMA−SA system were
217 taken as reference to discuss those of the PZ−SA system. The formation free energy

surface of the PZ−SA system obtained at the DLPNO-CCSD(T)/aug-cc-pVTZ level of theory and 278.15 K was shown in Figure 2A, and the corresponding formation free energy surface at 298.15 K, ΔH and ΔS values were presented in SI. A comparison for the formation free energies at the ωB97X-D/6-31++G(d,p) level and the DLPNO-CCSD(T)/aug-cc-pVTZ level was presented in SI. As can be seen in Figure 2A, the ΔG values for all the PZ−SA clusters are lower than those of the corresponding DMA−SA clusters,[70] implying a high enhancing potential of PZ on SA-based NPF. The lower ΔG values of all PZ−SA clusters relative to the corresponding DMA−SA clusters are consistent with the order of their GB values (PZ > DMA). Therefore, the GB plays a determining role in the ΔG values of PZ−SA clusters, agreeing well with recent finding on the importance of the GB in the ΔG values for < 2 nm amine-SA clusters.[55,103]

For the potential use of PZ as an alternative solvent to MEA in PCCC applications, it is interesting to compare the ΔG values of PZ−SA with the MEA−SA systems. It was found that ΔG values of the majority of the PZ−SA clusters are lower than those of the corresponding MEA−SA clusters with the exception of the $(PZ)_{2\text{-}4}$ and $(PZ)_1(SA)_{3\text{-}4}$ clusters. This exception illustrates the important role of the –OH group of MEA in the formation of MEA−SA clusters as presented in our previous study.[70]

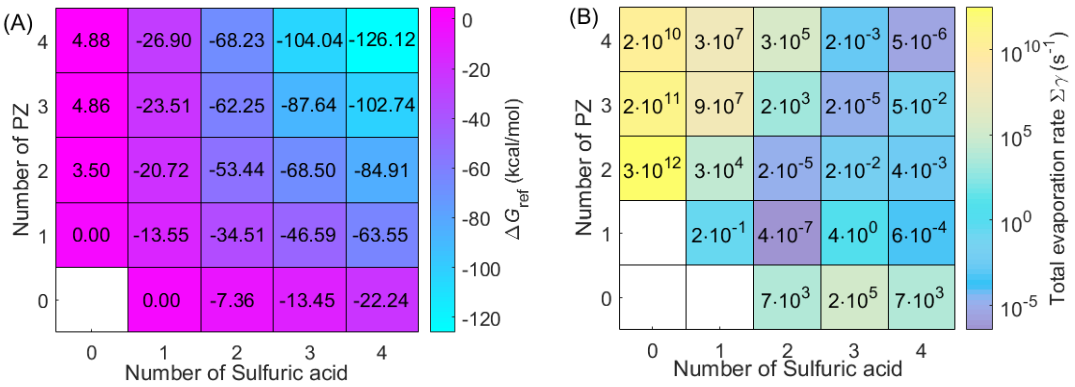

Figure 2. Calculated formation free energies (ΔG) (A) for $(PZ)_x(SA)_y$ clusters (x = 0−4, y = 0−4) at the DLPNO-CCSD(T)/aug-cc-pVTZ//ωB97X-D/6-31++G(d,p) level of theory and corresponding total evaporation rates (B) for each cluster at 278.15 K and

238 the reference pressure of PZ and SA is set to 1 atm.

239 **Evaporation Rates and Cluster Stability.** Comparing the evaporation rate of a cluster
240 to the growth rate due to the collisions with vapor molecules at the given acid and base
241 concentration yields a measure of the stability of the cluster against evaporation. The
242 calculated evaporation rates of all PZ−SA clusters at 278.15 K were presented in Figure
243 2B. According to the condition judging the stability of a cluster (the cluster with
244 evaporation rate lower than 10^{-3} s^{-1} is stable when the concentration of acid or base
245 monomer is around or above ppt level), only $(PZ)_1(SA)_2$, $(PZ)_1(SA)_4$, $(PZ)_2(SA)_2$,
246 $(PZ)_2(SA)_4$, $(PZ)_3(SA)_3$, $(PZ)_4(SA)_3$, and $(PZ)_4(SA)_4$ clusters can be considered stable
247 enough against evaporation. The three clusters along the diagonal ($(PZ)_2(SA)_2$,
248 $(PZ)_3(SA)_3$, $(PZ)_4(SA)_4$) as well as the $(PZ)_1(SA)_2$ clusters are the most stable with
249 evaporation rates of 10^{-5}−10^{-7} s^{-1}. In addition, the clusters $(PZ)_2(SA)_3$ and $(PZ)_3(SA)_4$
250 are relatively stable with evaporation rates in the order of 10^{-2} s^{-1}. By checking the
251 evaporation rates for all possible evaporation pathways of each of the PZ−SA clusters
252 (Table S3), it was found that the main decay route for all PZ−SA clusters (except
253 clusters $(PZ)_4(SA)_{2\text{-}4}$) is via evaporation of a PZ or SA monomer. A detailed discussion
254 on the main decay routes for all PZ−SA clusters were presented in SI.

255 It is also interesting to compare cluster evaporation rates for the different amines
256 (MEA, DMA, PZ and PUT) at the same simulation conditions. Generally, most of the
257 PZ−SA clusters have lower evaporation rates than the corresponding
258 DMA/MEA/PUT−SA clusters.[70,78] For the number of clusters with evaporation rates
259 less than or around 10^{-3} s^{-1}, the PZ−SA system is equal to that of the PUT−SA system
260 and higher than the MEA/DMA−SA systems. The PZ−SA system has more clusters
261 with evaporation rates less than or around 10^{-5} s^{-1} than any other amines-SA systems.
262 This indicates that the PZ−SA system has more stable clusters than the MEA/DMA−SA

263 systems and more high stable clusters than the PUT−SA system. In addition, these
264 stable clusters for the PZ−SA system are more even-distributed among the clusters with
265 different size than those of other systems. The above results do not necessarily
266 guarantee the faster growth of PZ−SA system compared to the DMA/MEA/PUT−SA
267 systems. However, the higher number of stable clusters will facilitate the growth of the
268 PZ−SA system once the crucial PZ−SA cluster is formed. When the initially formed
269 one SA and one base cluster, which are crucial for cluster growth at relevant SA and
270 base concentration for PZ−SA (see Section Growth Pathway), DMA−SA, MEA−SA
271 and PUT−SA systems,[69,70,78] are compared, the trend in evaporation rate follows
272 $(PUT)_1(SA)_1 > (PZ)_1(SA)_1 > (DMA)_1(SA)_1 > (MEA)_1(SA)_1$ at the given acid and base
273 concentrations.[70,78]
274 **Steady-State Cluster Concentrations and Formation Rates.** The cluster formation
275 rates (J_{PZ}) and steady-state sulfuric acid dimer concentrations ($\sum_i[(SA)_2(PZ)_i]$) as a
276 function of the concentration of SA (10^5−10^8 cm^{-3}) and PZ (1−100 ppt) for the PZ−SA
277 system at 278.15 K were presented in Figure 3. The comparison with the DMA−SA
278 (J_{DMA}, $\sum_i[(SA)_2(DMA)_i]$), PUT−SA (J_{PUT}, $\sum_i[(SA)_2(PUT)_i]$) and MEA−SA (J_{MEA},
279 $\sum_i[(SA)_2(MEA)_i]$) cluster systems were shown in Figure S3. As can be seen in Figure
280 3, with increasing [SA] and [PZ], J_{PZ} and $\sum_i[(SA)_2(PZ)_i]$ gradually increase. As the
281 [PZ] increases, $\sum_i[(SA)_2(PZ)_i]$ becomes saturated. More importantly, the J_{PZ} is 1−10^3,
282 8−10^3 and 0.02−0.9 times that of J_{DMA}, J_{MEA} and J_{PUT}, respectively, and
283 $\sum_i[(SA)_2(PZ)_i]$ is 0.7−2, 5−80 and 0.08−0.9 times that of $\sum_i[(SA)_2(DMA)_i]$,
284 $\sum_i[(SA)_2(MEA)_i]$ and $\sum_i[(SA)_2(PUT)_i]$, respectively, depending on the
285 concentration of SA and amines. The enhancing potential of these four amines follows

286 the order PUT > PZ > DMA > MEA, consistent with the order of their GB values (PUT
287 954.3, PZ 914.7, DMA 896.5, MEA 896.8 kJ mol^{-1}) except for MEA. In addition, both
288 J_{PZ} and $\sum_i[(SA)_2(PZ)_i]$ present a negative temperature dependence in temperature
289 range of 258.15−313.15 K (Figure S4), similar to the case of the MEA−SA system.[70]

290 We noted that ambient observations and experiments have shown that DMA is a
291 dominant enhancing agent for SA-based NPF at 5−10 ppt level although its atmospheric
292 concentration is 2-3 orders magnitude lower than that of ammonia and similar to or a
293 little lower than other atmospheric amines.[1,62,71,104] In ambient observations and
294 experiments, coexisting amines with DMA mainly included monoamines.[2-4] With our
295 computational data, the required concentration of PZ, which can lead to a similar
296 enhancing effect of 5−10 ppt DMA on SA-based NPF at 278.15 K, is estimated. It is
297 found that 2−4 ppt PZ ([SA] =10^7 cm^{-3}) and 1.5−3 ppt PZ ([SA] =10^6 cm^{-3}) yield a
298 similar enhancing effect as 5-10 ppt DMA. Therefore, it can be concluded that PZ can
299 significantly enhance SA-based NPF when the atmospheric [PZ] reaches ppt level, a
300 similar concentration as measured in the Zonguldak province, Turkey.[76] These findings
301 imply that if PZ is used as PCCC solvent, local discharges will lead to a high potential
302 to form new particles in the atmosphere.

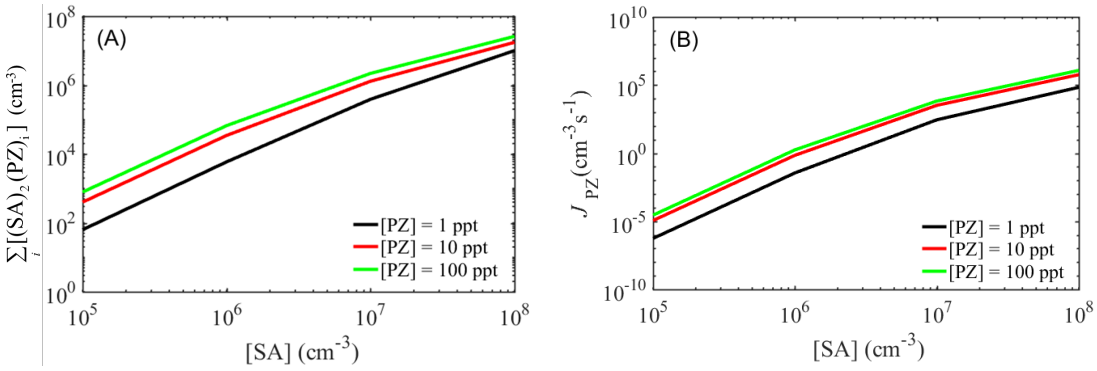

303 Figure 3. Simulated steady-state SA dimer concentration $\sum_i[(SA)_2(PZ)_i]$ (cm^{-3}) (A)
304 and the cluster formation rates J_{PZ} (cm^{-3} s^{-1}) out of the simulation systems (B) as a

function of [PZ] at 278.15 K.

Growth Pathways. The growth pathway and actual Gibbs free energy surface for the PZ−SA clusters at 278.15 K, [SA] = 10^6 cm^{-3} and [PZ] = 10 ppt were shown in Figure 4. As can be seen in Figure 4A, the first step of the PZ−SA system growth is the formation of the $(PZ)_1(SA)_1$ cluster, similar to the cases of the MEA−SA and DMA−SA systems.[70] The growth of the formed $(PZ)_1(SA)_1$ cluster mainly proceeds by first adding one SA molecule, and then one PZ molecule until the formation of $(PZ)_3(SA)_3$ cluster. This mechanism is similar to the case of the MEA−SA system.[70] However, different from MEA−SA system, the $(PZ)_3(SA)_3$ cluster growth mainly proceeds by first adding one PZ molecule, and then one SA molecule to form $(PZ)_4(SA)_4$ cluster. Collisions with the $(PZ)_1(SA)_1$ cluster, instead of PZ or SA molecule, contributes 20-33% to the formation of $(PZ)_2(SA)_2$, $(PZ)_3(SA)_3$ and $(PZ)_4(SA)_4$ clusters. $(PZ)_4(SA)_5$ (57%) is main cluster leaving the simulation box, followed by $(PZ)_5(SA)_5$ (24%), $(PZ)_6(SA)_5$ (10%) and other clusters (9%). Combining the growth pathway with the actual Gibbs free energy surface (Figure 4B), it can be seen that only the cluster $(PZ)_2(SA)_2 \rightarrow (PZ)_2(SA)_3$ process needs to overcome a small barrier, whereas the remaining processes along the main growth pathway are barrierless after the formation of the $(PZ)_1(SA)_1$ cluster. However, the growth pathway via cluster collisions with $(PZ)_1(SA)_1$ cluster along the diagonal is barrierless along the entire growth pathway. Combining the growth pathway with the evaporation rate of the PZ−SA system, we conclude that the formation of initial $(PZ)_1(SA)_1$ cluster is the rate determining step for the cluster growth due to its instability compared with other clusters in the growth pathway, similar to cases of clusters containing SA and other amines including MA, MEA and DMA.[70]

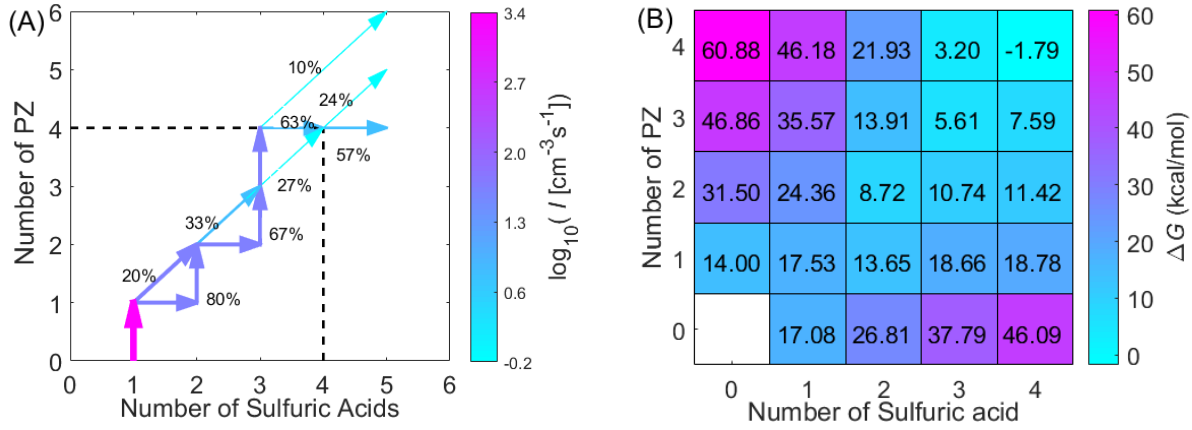

328 Figure 4. Main clustering pathways (A) and actual Gibbs free energy surface (B) for
329 the formation of clusters $(PZ)_x(SA)_y$ (x = 0−4, y = 0−4) at 278.15 K, [SA] = 10^6 cm^{-3},
330 and [PZ] = 10 ppt.

331 **Hydration Effect.** We considered 1−5 H_2O molecules to study the effect of hydration
332 on the formation kinetics of the PZ−SA clusters. It should be noted that only clusters
333 $(PZ)_x(SA)_y$ (x = 0−2, y = 0−2) were considered as a test to investigate the effect of
334 hydration as the computational cost increasing rapidly when studying larger clusters.
335 Details for the discussion on the calculated stepwise hydration free energies and the
336 optimized conformations of the hydrated PZ-SA clusters were presented in the SI. The
337 calculated equilibrium hydrate distributions of the clusters at 278.15 K and relative
338 humidities (RH) 20%, 50% and 80% were presented in Figure S5. Figure S5 shows that
339 the PZ−SA clusters are hydrated by less than three H_2O molecules depending on the
340 RH. The evaporation rates and formation rates compared to dry conditions as a function
341 of RH at 278.15 K were presented in Figure 5. Figure 5A shows that the effect of
342 hydration on the evaporation rates depends on the cluster composition. Hydration has
343 little effect on the $(SA)_2$ cluster and almost no effect on the $(PZ)_2$ and $(PZ)_2(SA)_2$
344 clusters. However, the evaporation rates of the $(PZ)_1(SA)_2$ and $(PZ)_2(SA)_1$ clusters can
345 be increased up to 50 and 190 times by hydration compared to the dry cases,
346 respectively. However, hydration can greatly decrease (up to 50 times) the evaporation

rate of the initially formed $(PZ)_1(SA)_1$ cluster, the rate-determining step for the cluster growth in the system. This is the main reason for the increase in the cluster formation rates (Figure 5B) when hydration is considered compared to the dry case. The cluster formation rates increase up to 2 times compared to the dry case. Therefore, from these small cluster hydration simulations, we can conclude that hydration has a significant effect on the evaporation rates and a minor effect on the formation rates.

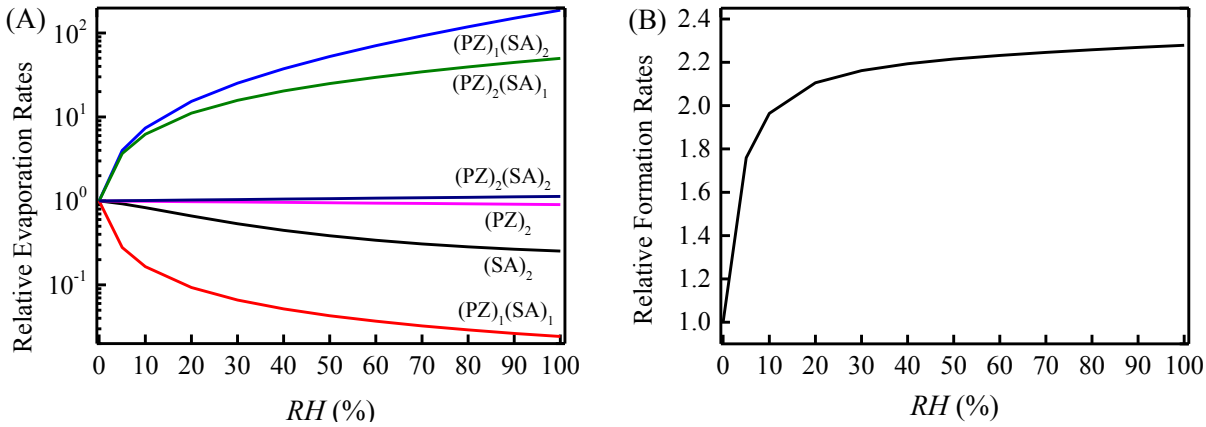

Figure 5. Relative evaporation rates (A) and cluster formation rates ([SA] = 10^6 cm^{-3} and [PZ] = 10 ppt) (B) as a function of relative humidities (*RH*) at 278.15 K.

Implications. We have revealed that PZ at ppt level can significantly enhance SA-based NPF. The enhancing potential of PZ is higher than that of DMA and MEA, and lower than that of PUT.[70,78] The order of the enhancing potential of the amines is consistent with that of their GB, further indicating the important role of GB of amines involved in SA-based NPF. In addition, we showed that the two –NH– groups of PZ cannot synergistically interact with SA, making PZ behave similarly to monoamines as opposed to chainlike diamines in stabilizing SA. In this way, one of the –NH– groups points outwards from the clusters. The existence of the exterior –NH– group on the surface of the clusters would make the subsequent growth mechanism of the PZ-SA nucleus different from other cases of amines-SA nucleation. It could be interesting to probe the further growth mechanism of PZ-SA nucleation in future by studying larger

366 cluster structures.

367 Obviously, the participation in SA-based NPF is one removal pathway for the
368 emitted PZ, similar to the case of MEA. The removal rate constants (k_{SA}) of PZ by
369 participating in SA-based NPF are estimated to be 3.2×10^{-10} and 4.0×10^{-10} cm^{-3}
370 $molecule^{-1}$ s^{-1} at 278.15 K at dry (RH = 0) and 50% RH conditions, respectively (SI).
371 Previous studies have shown that the reactions with ·OH and ·Cl are important removal
372 pathways for PZ at daytime, due to their high reaction rate constants ($k_{OH} = 2.7 \times 10^{-10}$
373 cm^{-3} $molecule^{-1}$ s^{-1}, $k_{Cl} = 4.7 \times 10^{-10}$ cm^{-3} $molecule^{-1}$ s^{-1}) at 278.15 K.[28,32] The three
374 reactive agents (·OH, ·Cl and SA) toward PZ can coexist in the atmosphere and the
375 concentration of ·Cl ([·Cl]) and [SA] is estimated to be around 0.01−0.1 and 1−19 times
376 of that of ·OH ([·OH]) during daytime, respectively.[105-110] Based on k_{SA}, k_{OH}, k_{Cl}, [SA],
377 [·OH] and [·Cl], we estimated the contribution of the participation in SA-based NPF
378 (Con_{SA}) to the removal of PZ by $k_{SA}[SA]/(k_{OH}[\cdot OH] + k_{Cl}[\cdot Cl] + k_{SA}[SA])$ at 278.15 K
379 and RH=0 or 50% (Table S6). As can be seen in Table S6, Con_{SA} is 50%-97%,
380 indicating the participation in SA-based NPF is a dominant removal pathway for PZ at
381 278.15 K, especially at high [SA]. It was found that the Con_{SA} to the removal of PZ has
382 a negative temperature dependence in temperature range of 258.15−313.15 K (Figure
383 S6). When the temperature effect is considered, the participation in SA-based NPF still
384 play an important role in removing PZ at all atmospheric conditions, except a combined
385 condition of low [SA], low RH and high temperature. Therefore, if ignoring the
386 participation of PZ in SA-based NPF, the contribution of atmospheric oxidation by ·OH
387 and ·Cl to the removal of PZ will be highly overestimated. In addition, the contribution
388 of the participation in SA-based NPF on PZ removal is higher than that to the MEA
389 removal at both 0 and 50% RH conditions, and 278.15 K (SI). More importantly, the
390 high contribution of the NPF pathway to the removal of PZ decreases the overall

391 nitrosamine yield compared to only considering the atmospheric ·OH and ·Cl oxidation
392 pathways. The higher contribution of the NPF pathway to the removal of PZ than that
393 to the removal of MEA decreases their relative risk of nitrosamine formation. A detailed
394 discussion on the reevaluation of the overall nitrosamine yield of PZ and MEA was
395 presented in SI. Therefore, this study further stresses that the participation in SA-based
396 NPF should be considered for other atmospheric amines to evaluate the environmental
397 risk, especially for the formation of carcinogenic nitrosamine.

398 **ASSOCIATED CONTENT**

399 **Supporting Information.** Details of the chosen boundary conditions, comparison for
400 the formation free energies at low and high theoretical level, observed number of proton
401 transfers in the PZ-SA system, stepwise hydration free energies, removal rate constants
402 of PZ by participating in SA-based NPF, main decay route for all PZ−SA clusters,
403 thermochemical information of PZ−SA clusters, ΔG values of PZ−SA clusters at
404 298.15 K, evaporation rates for all evaporation pathways of PZ−SA clusters, the cluster
405 formation rates and steady-state SA dimer concentrations as a function of temperature,
406 conformations of the hydrated PZ-SA clusters, hydrate distribution of studied clusters,
407 Con_{SA} to the removal of PZ and MEA, detailed discussion on the reevaluation of the
408 overall nitrosamine yield of PZ and MEA and coordinates of all optimized clusters.

409 **AUTHOR INFORMATION**

410 **Corresponding Author**

411 *Phone/fax: +86-411-84707251; E-mail: hbxie@dlut.edu.cn, jwchen@dlut.edu.cn

412 **ACKNOWLEDGEMENTS**

413 The study was supported by the National Natural Science Foundation of China
414 (21876024, 21677028), the Major International (Regional) Joint Research Project

(21661142001), the Program for Changjiang Scholars and Innovative Research Team in University (IRT_13R05), and the Programme of Introducing Talents of Discipline to Universities (B13012) and Supercomputing Center of Dalian University of Technology. J. E thanks the Villum Foundation for financial support. H. V. thanks the European Research Council (Grant No. 692891-DAMOCLES) and the University of Helsinki, Faculty of Science ATMATH project for funding.

REFERENCES

(1) Ge, X. L.; Wexler, A. S.; Clegg, S. L. Atmospheric amines - Part I. A review. *Atmos. Environ.* **2011**, 45, 524-546.

(2) Yao, L.; Wang, M. Y.; Wang, X. K.; Liu, Y. J.; Chen, H. F.; Zheng, J.; Nie, W.; Ding, A. J.; Geng, F.-H.; Wang, D. F.; Chen, J. M.; Worsnop, D. R.; Wang, L. Detection of atmospheric gaseous amines and amides by a high-resolution time-of-flight chemical ionization mass spectrometer with protonated ethanol reagent ions. *Atmos. Chem. Phys.* **2016**, 16, 14527-14543.

(3) Zheng, J.; Ma, Y.; Chen, M.; Zhang, Q.; Wang, L.; Khalizov, A. F.; Yao, L.; Wang, Z.; Wang, X.; Chen, L. Measurement of atmospheric amines and ammonia using the high resolution time-of-flight chemical ionization mass spectrometry. *Atmos. Environ.* **2015**, 102, 249-259.

(4) You, Y.; Kanawade, V. P.; de Gouw, J. A.; Guenther, A. B.; Madronich, S.; Sierra-Hernández, M. R.; Lawler, M.; Smith, J. N.; Takahama, S.; Ruggeri, G.; Koss, A.; Olson, K.; Baumann, K.; Weber, R. J.; Nenes, A.; Guo, H.; Edgerton, E. S.; Porcelli, L.; Brune, W. H.; Goldstein, A. H.; Lee, S. H. Atmospheric amines and ammonia measured with a chemical ionization mass spectrometer (CIMS). *Atmos. Chem. Phys.* **2014**, 14, 12181-12194.

(5) Hemmilä, M.; Hellén, H.; Virkkula, A.; Makkonen, U.; Praplan, A. P.; Kontkanen, J.; Ahonen, L.; Kulmala, M.; Hakola, H. Amines in boreal forest air at SMEAR II station in Finland. *Atmos. Chem. Phys.* **2018**, 18, 6367-6380.

(6) Hong, Y.; Liu, Y. R.; Wen, H.; Miao, S. K.; Huang, T.; Peng, X. Q.; Jiang, S.; Feng, Y. J.; Huang, W. Interaction of oxalic acid with methylamine and its atmospheric implications. *RSC Adv.* **2018**, 8, 7225-7234.

(7) Mao, J. B.; Yu, F. Q.; Zhang, Y.; An, J. Y.; Wang, L.; Zheng, J.; Yao, L.; Luo, G.; Ma, W. C.; Yu, Q.; Huang, C.; Li, L.; Chen, L. M. High-resolution modeling of gaseous methylamines over a polluted region in China: source-dependent emissions and implications of spatial variations. *Atmos. Chem. Phys.* **2018**, 18, 7933-7950.

(8) van Pinxteren, M.; Fomba, K. W.; van Pinxteren, D.; Triesch, N.; Hoffmann, E. H.; Cree, C. H. L.; Fitzsimons, M. F.; von Tümpling, W.; Herrmann, H. Aliphatic amines at the Cape Verde Atmospheric Observatory: Abundance, origins and sea-air fluxes. *Atmos. Environ.* **2019**, 203, 183-195.

(9) Dawson, M. L.; Varner, M. E.; Perraud, V.; Ezell, M. J.; Wilson, J.; Zelenyuk, A.; Gerber, R. B.; Finlayson-Pitts, B. J. Amine–amine exchange in aminium–methanesulfonate aerosols. *J. Phys. Chem. C* **2014**, 118, 29431-29440.

(10) Chen, H.; Wang, M.; Yao, L.; Chen, J.; Wang, L. Uptake of gaseous alkylamides by suspended sulfuric acid particles: Formation of ammonium/aminium salts. *Environ. Sci. Technol.* **2017**, 51, 11710-11717..

(11) Marrero-Ortiz, W.; Hu, M.; Du, Z.; Ji, Y.; Wang, Y.; Guo, S.; Lin, Y.; Gomez-Hermandez, M.; Peng, J.; Li, Y.; Secrest, J.; Levy Zamora, M.; Wang, Y.; An, T.; Zhang, R. Formation and optical properties of brown carbon from small alpha-dicarbonyls and amines. *Environ. Sci. Technol.* **2018**, 53, 117-126.

(12) Kumar, M.; Li, H.; Zhang, X.; Zeng, X. C.; Francisco, J. S. Nitric acid-amine chemistry in the gas phase and at the air-water interface. *J. Am. Chem. Soc.* **2018**, 140, 6456-6466.

(13) Nielsen, C. J.; Herrmann, H.; Weller, C. Atmospheric chemistry and environmental impact of the use of amines in carbon capture and storage (CCS). *Chem. Soc. Rev.* **2012**, 41, 6684-6704.

(14) Zhu, L.; Schade, G. W.; Nielsen, C. J. Real-time monitoring of emissions from monoethanolamine-based industrial scale carbon capture facilities. *Environ. Sci. Technol.* **2013**, 47, 14306-14314.
(15) da Silva, G. Formation of nitrosamines and alkyldiazohydroxides in the gas phase: the CH_3NH + NO reaction revisited. *Environ. Sci. Technol.* **2013**, 47, 7766-7772.
(16) Borduas, N.; Murphy, J. G.; Wang, C.; da Silva, G.; Abbatt, J. P. D. Gas phase oxidation of nicotine by OH radicals: kinetics, mechanisms, and formation of HNCO. *Environ. Sci. Technol. Lett.* **2016**, 3, 327-331.
(17) Xie, H. B.; Li, C.; He, N.; Wang, C.; Zhang, S. W.; Chen, J. W. Atmospheric chemical reactions of monoethanolamine initiated by OH radical: mechanistic and kinetic study. *Environ. Sci. Technol.* **2014**, 48, 1700-1706.
(18) Xie, H. B.; Ma, F. F.; Wang, Y. F.; He, N.; Yu, Q.; Chen, J. W. Quantum chemical study on ·Cl-initiated atmospheric degradation of monoethanolamine. *Environ. Sci. Technol.* **2015**, 49, 13246-13255.
(19) Xie, H. B.; Ma, F. F.; Yu, Q.; He, N.; Chen, J. W. Computational study of the reactions of chlorine radicals with atmospheric organic compounds featuring NH_x-pi-bond (x = 1, 2) structures. *J. Phys. Chem. A* **2017**, 121, 1657-1665.
(20) Onel, L.; Thonger, L.; Blitz, M. A.; Seakins, P. W.; Bunkan, A. J.; Solimannejad, M.; Nielsen, C. J. Gas-phase reactions of OH with methyl amines in the presence or absence of molecular oxygen. an experimental and theoretical study. *J. Phys. Chem. A* **2013**, 117, 10736-10745.
(21) Tan, W.; Zhu, L.; Mikoviny, T.; Nielsen, C. J.; Wisthaler, A.; Eichler, P.; Muller, M.; D'Anna, B.; Farren, N. J.; Hamilton, J. F.; Pettersson, J. B. C.; Hallquist, M.; Antonsen, S.; Stenstrom, Y. Theoretical and experimental study on the reaction of tert-Butylamine with OH radicals in the atmosphere. *J. Phys. Chem. A* **2018**, 122, 4470-4480.
(22) Barnes, I.; Wiesen, P.; Gallus, M. Rate coefficients for the reactions of OH radicals with a series of alkyl-substituted amines. *J. Phys. Chem. A* **2016**, 120, 8823-8829.
(23) Onel, L.; Blitz, M. A.; Breen, J.; Rickard, A. R.; Seakins, P. W. Branching ratios for the reactions of OH with ethanol amines used in carbon capture and the potential impact on carcinogen formation in the emission plume from a carbon capture plant. *Phys. Chem. Chem. Phys.* **2015**, 17, 25342-25353.
(24) Onel, L.; Blitz, M.; Dryden, M.; Thonger, L.; Seakins, P. Branching ratios in reactions of OH radicals with methylamine, dimethylamine, and ethylamine. *Environ. Sci. Technol.* **2014**, 48, 9935-9942.
(25) Nicovich, J. M.; Mazumder, S.; Laine, P. L.; Wine, P. H.; Tang, Y.; Bunkan, A. J.; Nielsen, C. J. An experimental and theoretical study of the gas phase kinetics of atomic chlorine reactions with CH_3NH_2, $(CH_3)_2NH$, and $(CH_3)_3N$. *Phys. Chem. Chem. Phys.* **2015**, 17, 911-917.
(26) Borduas, N.; Abbatt, J. P.; Murphy, J. G.; So, S.; da Silva, G. Gas-phase mechanisms of the reactions of reduced organic nitrogen compounds with OH radicals. *Environ. Sci. Technol.* **2016**, 50, 11723-11734.
(27) Borduas, N.; da Silva, G.; Murphy, J. G.; Abbatt, J. P. D. Experimental and theoretical understanding of the gas phase oxidation of atmospheric amides with OH radicals: kinetics, products, and mechanisms. *J. Phys. Chem. A* **2015**, 119, 4298-4308.
(28) Onel, L.; Dryden, M.; Blitz, M. A.; Seakins, P. W. Atmospheric oxidation of piperazine by OH has a low potential to form carcinogenic compounds. *Environ. Sci. Technol. Lett.* **2014**, 1, 367-371.

(29) Sarma, P. J.; Gour, N. K.; Bhattacharjee, D.; Mishra, B. K.; Deka, R. C. Hydrogen atom abstraction from piperazine by hydroxyl radical: a theoretical investigation. *Mol. Phys.* **2017**, 115, 962-970.
(30) Borduas, N.; Abbatt, J. P.; Murphy, J. G. Gas phase oxidation of monoethanolamine (MEA) with OH radical and ozone: kinetics, products, and particles. *Environ. Sci. Technol.* **2013**, 47, 6377-6383.
(31) Onel, L.; Blitz, M. A.; Seakins, P. W. Direct determination of the rate coefficient for the reaction of OH radicals with monoethanol amine (MEA) from 296 to 510 K. *J. Phys. Chem. Lett.* **2012**, 3, 853-856.
(32) Ma, F. F.; Ding, Z. Z.; Elm, J.; Xie, H. B.; Yu, Q.; Liu, C.; Li, C.; Fu, Z. Q.; Zhang, L. L.; Chen, J. W. Atmospheric oxidation of piperazine initiated by ·Cl: unexpected high nitrosamine yield. *Environ. Sci. Technol.* **2018**, 52, 9801-9809.
(33) Nielsen, C. J.; D´Anna, B.; Bossi, R.; Bunkan, A. J. C.; Dithmer, L.; Glasius, M.; Hallquist, M.; Hansen, A. M. K.; Lutz, A.; Salo, K.; Maguta, M. M.; Nguyen, Q.; Mikoviny, T.; Müller, M.; Skov, H.; Sarrasin, E.; Stenstrøm, Y.; Tang, Y.; Westerlund, J.; Wisthaler, A. Atmospheric degradation of amines (ADA). *ISBN 978-82-992954-7-5, http://urn.nb.no/URN:NBN:no 30510,University of Oslo, Oslo,* **2012**.
(34) Olszyna, K.; Heicklen, J. The inhibition of photochemical smog-Vl. The reaction of O_3 with diethyihydroxylamin. *Sci. Total Environ*. **1976**, 5, 223-230.
(35) Atkinson, R.; Perry, R. A.; Pitts, J. N. Rate constants for the reaction of the OH radical with CH_3SH and CH_3NH_2 over the temperature range 299-426 K. *J. Chem. Phys.* **1977**, 66, 1578-1581.
(36) Atkinson, R.; Perry, R. A.; Pitts, J. N. Rate constants for the reactions of the OH radical with $(CH_3)_2NH$, $(CH_3)_3N$, and $C_2H_5NH_2$ over the temperature range 298-426 K. *J. Chem. Phys.* **1978**, 68, 1850-1853.
(37) Harris, G. W.; Atkinson, R.; Pitts, J. N. Kinetics of the reactions of the hydroxyl radical with hydrazine and methylhydrazine. *J. Chem. Phys.* **1979**, 83, 2557-2559.
(38) Harris, G. W.; Pitts, J. N. Notes. Rates of reaction of hydroxyl radicals with 2-(dimethylamino)ethanol and 2-amino-2-methyl-1-propanol in the gas phase at 300 ± 2 K. *Environ. Sci. Technol.* **1983**, 17, 50-51.
(39) Gleim, J.; Heicklen, J. The oxidation of diethylhydroxylamine by NO_2. *Int. J. Chem. Kinet*. **1982**, 14, 699-710.
(40) Lv, C. L.; Liu, Y. D.; Zhong, R.; Wang, Y. Theoretical studies on the formation of N-nitrosodimethylamine. *J. Mol. Struct.: THEOCHEM* **2007**, 802, 1-6.
(41) Hanst, P. L.; Spence, J. W.; Miller, M. Atmospheric chemistry of N-nitroso dimethylamine. *Environ. Sci. Technol.* **1977**, 11, 403-405.
(42) Chen, H.; Ezell, M. J.; Arquero, K. D.; Varner, M. E.; Dawson, M. L.; Gerber, R. B.; Finlayson-Pitts, B. J. New particle formation and growth from methanesulfonic acid, trimethylamine and water. *Phys. Chem. Chem. Phys.* **2015**, 17, 13699-13709.
(43) Chen, H.; Varner, M. E.; Gerber, R. B.; Finlayson-Pitts, B. J. Reactions of methanesulfonic acid with amines and ammonia as a source of new particles in air. *J. Phys. Chem. B* **2016**, 120, 1526-1536.
(44) Xu, J.; Finlayson-Pitts, B. J.; Gerber, R. B. Proton transfer in mixed clusters of methanesulfonic acid, methylamine, and oxalic acid: implications for atmospheric particle formation. *J. Phys. Chem. A* **2017**, 121, 2377-2385.
(45) Arquero, K. D.; Xu, J.; Gerber, R. B.; Finlayson-Pitts, B. J. Particle formation and growth from oxalic acid, methanesulfonic acid, trimethylamine and water: a combined experimental and theoretical study. *Phys. Chem. Chem. Phys.* **2017**, 19, 28286-28301.

(46) Arquero, K. D.; Gerber, R. B.; Finlayson-Pitts, B. J. The role of oxalic acid in new particle formation from methanesulfonic acid, methylamine, and water. *Environ. Sci. Technol.* **2017**, 51, 2124-2130.
(47) Xu, J.; Perraud, V.; Finlayson-Pitts, B. J.; Gerber, R. B. Uptake of water by an acid-base nanoparticle: theoretical and experimental studies of the methanesulfonic acid-methylamine system. *Phys. Chem. Chem. Phys.* **2018**, 20, 22249-22259.
(48) Chen, H.; Finlayson-Pitts, B. J. New particle formation from methanesulfonic acid and amines/ammonia as a function of temperature. *Environ. Sci. Technol.* **2017**, 51, 243-252.
(49) Lin, Y.; Ji, Y.; Li, Y.; Secrest, J.; Xu, W.; Xu, F.; Wang, Y.; An, T.; Zhang, R. Interaction between dicarboxylic acid and sulfuric acid-base clusters enhances new particle formation. *Atmos. Chem. Phys. Discuss.* **2018**, 1-46. DOI: 10.5194/acp-2018-975
(50) Zhao, H.; Jiang, X.; Du, L. Contribution of methane sulfonic acid to new particle formation in the atmosphere. *Chemosphere* **2017**, 174, 689-699.
(51) Liu, L.; Li, H.; Zhang, H.; Zhong, J.; Bai, Y.; Ge, M.; Li, Z.; Chen, Y.; Zhang, X. The role of nitric acid in atmospheric new particle formation. *Phys. Chem. Chem. Phys.* **2018**, 20, 17406-17414.
(52) Chu, B. W.; Kerminen, V. M.; Bianchi, F.; Yan, C.; Petaja, T.; Kulmala, M. Atmospheric new particle formation in China. *Atmos. Chem. Phys.* **2019**, 19, 115-138.
(53) Glasoe, W. A.; Volz, K.; Panta, B.; Freshour, N.; Bachman, R.; Hanson, D. R.; McMurry, P. H.; Jen, C. Sulfuric acid nucleation: An experimental study of the effect of seven bases. *J. Geophys. Res-Atmos.* **2015**, 120, 1933-1950.
(54) Olenius, T.; Halonen, R.; Kurtén, T.; Henschel, H.; Kupiainen-Määttä, O.; Ortega, I. K.; Jen, C. N.; Vehkamäki, H.; Riipinen, I. New particle formation from sulfuric acid and amines: Comparison of monomethylamine, dimethylamine, and trimethylamine. *J. Geophys. Res-Atmos.* **2017**, 122, 7103-7118.
(55) Yu, H.; McGraw, R.; Lee, S. H. Effects of amines on formation of sub-3 nm particles and their subsequent growth. *Geophys. Res. Lett.* **2012**, 39, L02807.
(56) Kurtén, T.; Loukonen, V.; Vehkamäki, H.; Kulmala, M. Amines are likely to enhance neutral and ion-induced sulfuric acid-water nucleation in the atmosphere more effectively than ammonia. *Atmos. Chem. Phys.* **2008**, 8, 4095-4103.
(57) Erupe, M. E.; Viggiano, A. A.; Lee, S. H. The effect of trimethylamine on atmospheric nucleation involving H_2SO_4. *Atmos. Chem. Phys.* **2011**, 11, 4767-4775.
(58) Nadykto, A. B.; Herb, J.; Yu, F. Q.; Xu, Y. S. Enhancement in the production of nucleating clusters due to dimethylamine and large uncertainties in the thermochemistry of amine-enhanced nucleation. *Chem. Phys. Lett.* **2014**, 609, 42-49.
Nadykto, A. B.; Herb, J.; Yu, F. Q.; Xu, Y. S.; Nazarenko, E. S. Estimating the lower limit of the impact of amines on nucleation in the earth's atmosphere. *Entropy* **2015**, 17, 2764-2780.
(60) Paasonen, P.; Olenius, T.; Kupiainen, O.; Kurtén, T.; Petäjä, T.; Birmili, W.; Hamed, A.; Hu, M.; Huey, L. G.; Plass-Duelmer, C.; Smith, J. N.; Wiedensohler, A.; Loukonen, V.; McGrath, M. J.; Ortega, I. K.; Laaksonen, A.; Vehkamäki, H.; Kerminen, V. M.; Kulmala, M. On the formation of sulphuric acid -amine clusters in varying atmospheric conditions and its influence on atmospheric new particle formation. *Atmos. Chem. Phys.* **2012**, 12, 9113-9133.
(61) Jen, C. N.; McMurry, P. H.; Hanson, D. R. Stabilization of sulfuric acid dimers by ammonia, methylamine, dimethylamine, and trimethylamine. *J. Geophys. Res-Atmos.* **2014**, 119, 7502-7514.

(62) Almeida, J.; Schobesberger, S.; Kurten, A.; Ortega, I. K.; Kupiainen-Maatta, O.; Praplan, A. P.; Adamov, A.; Amorim, A.; Bianchi, F.; Breitenlechner, M.; David, A.; Dommen, J.; Donahue, N. M.; Downard, A.; Dunne, E.; Duplissy, J.; Ehrhart, S.; Flagan, R. C.; Franchin, A.; Guida, R.; Hakala, J.; Hansel, A.; Heinritzi, M.; Henschel, H.; Jokinen, T.; Junninen, H.; Kajos, M.; Kangasluoma, J.; Keskinen, H.; Kupc, A.; Kurten, T.; Kvashin, A. N.; Laaksonen, A.; Lehtipalo, K.; Leiminger, M.; Leppa, J.; Loukonen, V.; Makhmutov, V.; Mathot, S.; McGrath, M. J.; Nieminen, T.; Olenius, T.; Onnela, A.; Petaja, T.; Riccobono, F.; Riipinen, I.; Rissanen, M.; Rondo, L.; Ruuskanen, T.; Santos, F. D.; Sarnela, N.; Schallhart, S.; Schnitzhofer, R.; Seinfeld, J. H.; Simon, M.; Sipila, M.; Stozhkov, Y.; Stratmann, F.; Tome, A.; Trostl, J.; Tsagkogeorgas, G.; Vaattovaara, P.; Viisanen, Y.; Virtanen, A.; Vrtala, A.; Wagner, P. E.; Weingartner, E.; Wex, H.; Williamson, C.; Wimmer, D.; Ye, P.; Yli-Juuti, T.; Carslaw, K. S.; Kulmala, M.; Curtius, J.; Baltensperger, U.; Worsnop, D. R.; Vehkamäki, H.; Kirkby, J. Molecular understanding of sulphuric acid-amine particle nucleation in the atmosphere. *Nature* **2013**, 502, 359-363.

(63) Jen, C. N.; Bachman, R.; Zhao, J.; McMurry, P. H.; Hanson, D. R. Diamine-sulfuric acid reactions are a potent source of new particle formation. *Geophys. Res. Lett.* **2016**, 43, 867-873.

(64) Wang, C. Y.; Jiang, S.; Liu, Y. R.; Wen, H.; Wang, Z. Q.; Han, Y. J.; Huang, T.; Huang, W. Synergistic effect of ammonia and methylamine on nucleation in the earth's atmosphere. A Theoretical Study. *J. Phys. Chem. A* **2018**, 122, 3470-3479.

(65) Lv, S. S.; Miao, S. K.; Ma, Y.; Zhang, M. M.; Wen, Y.; Wang, C. Y.; Zhu, Y. P.; Huang, W. Properties and atmospheric implication of methylamine-sulfuric acid-water clusters. *J. Phys. Chem. A* **2015**, 119, 8657-8666.

(66) Ma, Y.; Chen, J.; Jiang, S.; Liu, Y.-R.; Huang, T.; Miao, S.-K.; Wang, C.-Y.; Huang, W. Characterization of the nucleation precursor (H_2SO_4–$(CH_3)_2NH$) complex: intra-cluster interactions and atmospheric relevance. *RSC Adv.* **2016**, 6, 5824-5836.

(67) Qiu, C.; Zhang, R. Multiphase chemistry of atmospheric amines. *Phys*. *Chem*. *Chem*. *Phys*. **2013**, 15, 5738-5752.

(68) Zhang, R.; Wang, G.; Guo, S.; Zamora, M. L.; Ying, Q.; Lin, Y.; Wang, W.; Hu, M.; Wang, Y. Formation of urban fine particulate matter. *Chem. Rev.* **2015**, 115, 3803-3855.

(69) Elm, J. Elucidating the Limiting Steps in Sulfuric Acid-Base New Particle Formation. *J. Phys. Chem. A* **2017**, 121, 8288-8295.

(70) Xie, H. B.; Elm, J.; Halonen, R.; Myllys, N.; Kurtén, T.; Kulmala, M.; Vehkamäki, H. Atmospheric Fate of Monoethanolamine: Enhancing new particle formation of sulfuric acid as an important removal process. *Environ. Sci. Technol.* **2017**, 51, 8422-8431.

(71) Yao, L.; Garmash, O.; Bianchi, F.; Zheng, J.; Yan, C.; Kontkanen, J.; Junninen, H.; Mazon, S. B.; Ehn, M.; Paasonen, P.; Sipila, M.; Wang, M. Y.; Wang, X. K.; Xiao, S.; Chen, H. F.; Lu, Y. Q.; Zhang, B. W.; Wang, D. F.; Fu, Q. Y.; Geng, F. H.; Li, L.; Wang, H. L.; Qiao, L. P.; Yang, X.; Chen, J. M.; Kerminen, V. M.; Petaja, T.; Worsnop, D. R.; Kulmala, M.; Wang, L. Atmospheric new particle formation from sulfuric acid and amines in a Chinese megacity. *Science* **2018**, 361, 278.

(72) Ma, X.; Sun, Y.; Huang, Z.; Zhang, Q.; Wang, W. A density functional theory study of the molecular interactions between a series of amides and sulfuric acid. *Chemosphere* **2019**, 214, 781-790.

(73) Rochelle, G.; Chen, E.; Freeman, S.; Van Wagener, D.; Xu, Q.; Voice, A. Aqueous piperazine as the new standard for CO_2 capture technology. *Chem. Eng. J.* **2011**, 171, 725-733.

(74) Fine, N. A.; Nielsen, P. T.; Rochelle, G. T. Decomposition of nitrosamines in CO_2 capture by aqueous piperazine or monoethanolamine. *Environ. Sci. Technol.* **2014**, 48, 5996-6002.
(75) *Kirk-Othmer Encyclopedia of chemical technology*, 3rd ed., Vols 1-26. John Wiley and Sons: New York, NY, 1978-1984; 1978; Vol. V2, p296.
(76) Akyüz, M. Simultaneous determination of aliphatic and aromatic amines in ambient air and airborne particulate matters by gas chromatography-mass spectrometry. *Atmos. Environ.* **2008**, 42, 3809-3819.
(77) Hunter, E. P. L.; Lias, S. G. Evaluated gas phase basicities and proton affinities of molecules: An update. *J. Phys. Chem. Ref. Data* **1998**, 27, 413-656.
(78) Elm, J.; Passananti, M.; Kurtén, T.; Vehkamäki, H. Diamines can initiate new particle formation in the atmosphere. *J. Phys. Chem. A* **2017**, 121, 6155-6164.
(79) Olenius, T.; Kupiainen-Maatta, O.; Ortega, I. K.; Kurtén, T.; Vehkamaki, H. Free energy barrier in the growth of sulfuric acid-ammonia and sulfuric acid-dimethylamine clusters. *J. Chem. Phys.* **2013**, 139, 084312.
(80) McGrath, M. J.; Olenius, T.; Ortega, I. K.; Loukonen, V.; Paasonen, P.; Kurtén, T.; Kulmala, M.; Vehkamäki, H. Atmospheric cluster dynamics code: a flexible method for solution of the birth-death equations. *Atmos. Chem. Phys.* **2012**, 12, 2345-2355.
(81) Ortega, I. K.; Kupiainen, O.; Kurtén, T.; Olenius, T.; Wilkman, O.; McGrath, M. J.; Loukonen, V.; Vehkamäki, H. From quantum chemical formation free energies to evaporation rates. *Atmos. Chem. Phys.* **2012**, 12, 225-235.
(82) Shi, X.; Zhang, R.; Sun, Y.; Xu, F.; Zhang, Q.; Wang, W. A density functional theory study of aldehydes and their atmospheric products participating in nucleation. *Phys. Chem. Chem. Phys.* **2018**, 20, 1005-1011.
(83) Elm, J.; Jen, C. N.; Kurtén, T.; Vehkamäki, H. Strong hydrogen bonded molecular interactions between atmospheric diamines and sulfuric acid. *J. Phys. Chem. A* **2016**, 120, 3693-3700.
(84) Myllys, N.; Ponkkonen, T.; Passananti, M.; Elm, J.; Vehkamäki, H.; Olenius, T. Guanidine: A highly efficient stabilizer in atmospheric new-particle formation. *J. Phys. Chem. A* **2018**, 122, 4717-4729.
(85) Myllys, N.; Olenius, T.; Kurtén, T.; Vehkamäki, H.; Riipinen, I.; Elm, J. Effect of bisulfate, ammonia, and ammonium on the clustering of organic acids and sulfuric Acid. *J. Phys. Chem. A* **2017**, 121, 4812-4824.
(86) Elm, J.; Myllys, N.; Hyttinen, N.; Kurtén, T. Computational study of the clustering of a cyclohexene autoxidation product $C_6H_8O_7$ with itself and sulfuric acid. *J. Phys. Chem. A* **2015**, 119, 8414-8421.
(87) Li, H.; Zhong, J.; Vehkamäki, H.; Kurtén, T.; Wang, W.; Ge, M.; Zhang, S.; Li, Z.; Zhang, X.; Francisco, J. S.; Zeng, X. C. Self-catalytic reaction of SO_3 and NH_3 to produce sulfamic acid and its implication to atmospheric particle formation. *J. Am. Chem. Soc.* **2018**, 140, 11020-11028.
(88) Liu, L.; Kupiainen-Maatta, O.; Zhang, H.; Li, H.; Zhong, J.; Kurten, T.; Vehkamäki, H.; Zhang, S.; Zhang, Y.; Ge, M.; Zhang, X.; Li, Z. Clustering mechanism of oxocarboxylic acids involving hydration reaction: implications for the atmospheric models. *J. Chem. Phys.* **2018**, 148, 214303.
(89) F Frisch, M. J.; Trucks, G. W.; Schlegel, H. B.; Scuseria, G. E.; Robb, M. A.; Cheeseman, J. R.; Scalmani, G.; Barone, V.; Mennucci, B.; Petersson, G. A.; Nakatsuji, H.; Caricato, M.; Li, X.; Hratchian, H. P.; Izmaylov, A. F.; Bloino, J.; Zheng, G.; Sonnenberg, J. L.; Hada, M.; Ehara, M.; Toyota, K.; Fukuda, R.; Hasegawa, J.; Ishida, M.; Nakajima, T.; Honda, Y.; Kitao, O.; Nakai, H.; Vreven, T.; Montgomery, J. A., Jr.; Peralta, J. E.; Ogliaro, F.; Bearpark, M.; Heyd, J. J.; Brothers, E.; Kudin, K. N.;

714 Staroverov, V. N.; Kobayashi, R.; Normand, J.; Raghavachari, K.; Rendell, A.; Burant,
715 J. C.; Iyengar, S. S.; Tomasi, J.; Cossi, M.; Rega, N.; Millam, J. M.; Klene, M.; Knox,
716 J. E.; Cross, J. B.; Bakken, V.; Adamo, C.; Jaramillo, J.; Gomperts, R.; Stratmann, R.
717 E.; Yazyev, O.; Austin, A. J.; Cammi, R.; Pomelli, C.; Ochterski, J. W.; Martin, R. L.;
718 Morokuma, K.; Zakrzewski, V. G.; Voth, G. A.; Salvador, P.; Dannenberg, J. J.;
719 Dapprich, S.; Daniels, A. D.; Farkas, O.; Foresman, J. B.; Ortiz, J. V.; Cioslowski, J.;
720 Fox, D. J. *Gaussian 09*; Gaussian, Inc.: Wallingford, CT, 2009.
721 (90) Neese, F. The ORCA program system. *Wiley Interdiscip. Rev. Comput. Mol. Sci.*
722 **2012**, 2, 73-78.
723 (91) Elm, J.; Kristensen, K. Basis set convergence of the binding energies of strongly
724 hydrogen-bonded atmospheric clusters. *Phys. Chem. Chem. Phys.* **2017**, 19, 1122-1133.
725 (92) Elm, J.; Bilde, M.; Mikkelsen, K. V. Assessment of binding energies of
726 atmospherically relevant clusters. *Phys. Chem. Chem. Phys.* **2013**, 15, 16442-16445.
727 (93) Loukonen, V.; Kurtén, T.; Ortega, I. K.; Vehkamäki, H.; Padua, A. A. H.; Sellegri,
728 K.; Kulmala, M. Enhancing effect of dimethylamine in sulfuric acid nucleation in the
729 presence of water - a computational study. *Atmos. Chem. Phys.* **2010**, 10, 4961-4974.
730 (94) Kerminen, V. M.; Petäjä, T.; Manninen, H. E.; Paasonen, P.; Nieminen, T.; Sipilä,
731 M.; Junninen, H.; Ehn, M.; Gagné, S.; Laakso, L.; Riipinen, I.; Vehkamäki, H.; Kurten,
732 T.; Ortega, I. K.; Dal Maso, M.; Brus, D.; Hyvärinen, A.; Lihavainen, H.; Leppä, J.;
733 Lehtinen, K. E. J.; Mirme, A.; Mirme, S.; Hõrrak, U.; Berndt, T.; Stratmann, F.; Birmili,
734 W.; Wiedensohler, A.; Metzger, A.; Dommen, J.; Baltensperger, U.; Kiendler-Scharr,
735 A.; Mentel, T. F.; Wildt, J.; Winkler, P. M.; Wagner, P. E.; Petzold, A.; Minikin, A.;
736 Plass-Dülmer, C.; Pöschl, U.; Laaksonen, A.; Kulmala, M. Atmospheric nucleation:
737 highlights of the EUCAARI project and future directions. *Atmos. Chem. Phys.* **2010**,
738 10, 10829-10848.
739 (95) Kürten, A.; Li, C.; Bianchi, F.; Curtius, J.; Dias, A.; Donahue, N. M.; Duplissy, J.;
740 Flagan, R. C.; Hakala, J.; Jokinen, T.; Kirkby, J.; Kulmala, M.; Laaksonen, A.;
741 Lehtipalo, K.; Makhmutov, V.; Onnela, A.; Rissanen, M. P.; Simon, M.; Sipilä, M.;
742 Stozhkov, Y.; Tröstl, J.; Ye, P.; McMurry, P. H. New particle formation in the sulfuric
743 acid–dimethylamine–water system: reevaluation of CLOUD chamber measurements
744 and comparison to an aerosol nucleation and growth model. *Atmos. Chem. Phys.* **2018**,
745 18, 845-863.
746 (96) Tomicic, M.; Bødker Enghoff, M.; Svensmark, H. Experimental study of H_2SO_4
747 aerosol nucleation at high ionization levels. *Atmos. Chem. Phys.* **2018**, 18, 5921-5930.
748 (97) Zhang, R. Y. Getting to the critical nucleus of aerosol formation. *Science* **2010**,
749 328, 1366-1367.
750 (98) Kontkanen, J.; Lehtipalo, K.; Ahonen, L.; Kangasluoma, J.; Manninen, H. E.;
751 Hakala, J.; Rose, C.; Sellegri, K.; Xiao, S.; Wang, L.; Qi, X.; Nie, W.; Ding, A.; Yu,
752 H.; Lee, S.; Kerminen, V.-M.; Petäjä, T.; Kulmala, M. Measurements of sub-3 nm
753 particles using a particle size magnifier in different environments: from clean mountain
754 top to polluted megacities. *Atmos. Chem. Phys.* **2017**, 17, 2163-2187.
755 (99) Maso, M. D.; Hyvärinen, A.; Komppula, M.; Tunved, P.; Kerminen, V.-M.;
756 Lihavainen, H.; Öviisanen, Y.; Hansson, H.-C.; Kulmala, M. Annual and interannual
757 variation in boreal forest aerosol particle number and volume concentration and their
758 connection to particle formation. *Tellus B* **2017**, 60, 495-508.
759 (100) Henschel, H.; Kurtén, T.; Vehkamaki, H. Computational study on the effect of
760 hydration on new particle formation in the sulfuric acid/ammonia and sulfuric
761 acid/dimethylamine systems. *J. Phys. Chem. A* **2016**, 120, 1886-1896.
762 (101) Li, S.; Qu, K.; Zhao, H.; Ding, L.; Du, L. Clustering of amines and hydrazines in
763 atmospheric nucleation. *Chem. Phys.* **2016**, 472, 198-207.

(102) Ling, J.; Ding, X.; Li, Z.; Yang, J. First-principles study of molecular clusters formed by nitric acid and ammonia. *J. Phys. Chem. A* **2017**, 121, 661-668.
(103) Temelso, B.; Morrison, E. F.; Speer, D. L.; Cao, B. C.; Appiah-Padi, N.; Kim, G.; Shields, G. C. Effect of mixing ammonia and alkylamines on sulfate aerosol formation. *J. Phys. Chem. A* **2018**, 122, 1612-1622.
(104) Yu, F.; Luo, G. Modeling of gaseous methylamines in the global atmosphere: impacts of oxidation and aerosol uptake. *Atmos. Chem. Phys.* **2014**, 14, 12455-12464.
(105) Wang, D. Y. S.; Hildebrandt Ruiz, L. Secondary organic aerosol from chlorine-initiated oxidation of isoprene. *Atmos. Chem. Phys.* **2017**, 17, 13491-13508.
(106) Dhulipala, S. V.; Bhandari, S.; Hildebrandt Ruiz, L. Formation of oxidized organic compounds from Cl-initiated oxidation of toluene. *Atmos. Environ.* **2019**, 199, 265-273.
(107) Le Breton, M.; Hallquist, Å. M.; Pathak, R. K.; Simpson, D.; Wang, Y.; Johansson, J.; Zheng, J.; Yang, Y.; Shang, D.; Wang, H.; Liu, Q.; Chan, C.; Wang, T.; Bannan, T. J.; Priestley, M.; Percival, C. J.; Shallcross, D. E.; Lu, K.; Guo, S.; Hu, M.; Hallquist, M. Chlorine oxidation of VOCs at a semi-rural site in Beijing: significant chlorine liberation from $ClNO_2$ and subsequent gas- and particle-phase Cl–VOC production. *Atmos. Chem. Phys.* **2018**, 18, 13013-13030.
(108) Zheng, J.; Hu, M.; Zhang, R.; Yue, D.; Wang, Z.; Guo, S.; Li, X.; Bohn, B.; Shao, M.; He, L.; Huang, X.; Wiedensohler, A.; Zhu, T. Measurements of gaseous H_2SO_4 by AP-ID-CIMS during CAREBeijing 2008 Campaign. *Atmos. Chem. Phys.* **2011**, 11, 7755-7765.
(109) Berresheim, H. Gas-aerosol relationships of H_2SO_4, MSA, and OH: Observations in the coastal marine boundary layer at Mace Head, Ireland. *J. Geophys. Res.* **2002**, 107, 5-1−5-12.
(110) Wingenter, O. W.; Sive, B. C.; Blake, N. J.; Blake, D. R.; Rowland, F. S. Atomic chlorine concentrations derived from ethane and hydroxyl measurements over the equatorial Pacific Ocean: Implication for dimethyl sulfide and bromine monoxide. *J. Geophys. Res.-Atmos.* **2005**, 110, 10.